17
Compressible flow

Even if air and other gases appear to be quite compressible in our daily doings, we have until now only analyzed incompressible flow and sometimes applied it to gases. The reason is—as pointed out before—that a gas in steady flow "prefers to get out of the way" rather than become compressed when it encounters an obstacle. Unless one entraps the gas, for example in a balloon or bicycle tire, it will be effectively incompressible in steady flow as long as its velocity relative to obstacles and container walls is well below the speed of sound.

But when steady flow speeds approach the speed of sound, compression is unavoidable. At such speeds the air has, so to speak, not enough time to get out of the way. Normal passenger jets routinely cruise at speeds just below the speed of sound and considerable compression of air must be expected at the front end of the aircraft. High speed projectiles and fighter jets move at several times the speed of sound, while space vehicles and meteorites move at many times the speed of sound. At supersonic speeds, the compression at the front of a moving object becomes so strong that a pressure discontinuity or shock is formed which trails the object and is perceived as a sonic boom.

In unsteady flow the effective incompressibility of fluids cannot be counted on. Rapid changes in the boundary conditions will generate small-amplitude compression waves, called *sound*, in all fluids. When you clap your hands, you create momentarily a small disturbance in the air which propagates to your ear. The diaphragm of the loudspeaker in your radio vibrates in tune with the music carried by the radio waves and the electric currents in wires connecting it to the radio, and transfers these vibrations to the air where they continue as sound.

In this chapter we shall begin by investigating compressible flow in ideal fluids, first for harmonic sound waves, and next for sonic and supersonic steady flow through ducts and nozzles. The chapter ends with a discussion of the role of viscosity in compressible flow and the attenuation it causes in harmonic wave propagation.

17.1 Small-amplitude sound waves

Although harmonic compression waves propagate through the fluid at the speed of sound, the amplitude of the velocity oscillations in a sound wave is normally very small compared to the speed of sound. No significant bulk movement of air takes place over longer distances, but locally the air oscillates back and forth with small spatial amplitude, and the velocity, density and pressure fields oscillate along with it.

Wave equation for sound

The Euler equations for ideal compressible flow are obtained from the general dynamic equation (12.33) with stress tensor, $\sigma_{ij} = -p\delta_{ij}$, and the continuity equation (12.18) ,

$$\frac{\partial \boldsymbol{v}}{\partial t} + (\boldsymbol{v}\cdot\nabla)\boldsymbol{v} = \boldsymbol{g} - \frac{1}{\rho}\nabla p, \qquad \frac{\partial \rho}{\partial t} + \nabla\cdot(\rho\boldsymbol{v}) = 0, \tag{17.1}$$

The first expresses the local form of Newton's Second Law and the second local mass conservation. For simplicity we shall in this section assume that there are no volume forces (gravity), $\boldsymbol{g} = \boldsymbol{0}$ (see however problem 17.3).

Before any sound is produced the fluid is assumed to be in hydrostatic equilibrium with constant density ρ_0 and constant pressure p_0. We now disturb the equilibrium by setting the fluid into motion with a tiny velocity field $\boldsymbol{v}(\boldsymbol{x},t)$. This disturbance generates small changes in the density, $\rho = \rho_0 + \Delta\rho$, and the pressure, $p = p_0 + \Delta p$. Expanding to first order in the small quantities, $\boldsymbol{v}$, Δp, and $\Delta\rho$, the Euler equations become,

$$\frac{\partial \boldsymbol{v}}{\partial t} = -\frac{1}{\rho_0}\nabla\Delta p, \qquad \frac{\partial \Delta\rho}{\partial t} = -\rho_0\nabla\cdot\boldsymbol{v}. \tag{17.2}$$

Differentiating the second equation with respect to time and making use of the first, we get

$$\frac{\partial^2\Delta\rho}{\partial t^2} = \nabla^2\Delta p. \tag{17.3}$$

Assuming that the fluid obeys a barotropic equation of state, $p = p(\rho)$, we obtain a first-order relation between the pressure and density changes,

$$\Delta p = \left.\frac{dp}{d\rho}\right|_0 \Delta\rho = \frac{K_0}{\rho_0}\Delta\rho, \tag{17.4}$$

where K_0 is the equilibrium bulk modulus (defined in eq. (2.39) on page 32).

Eliminating $\Delta\rho$ in eq. (17.3) we get a *standard wave equation* for the pressure correction,

$$\boxed{\frac{1}{c_0^2}\frac{\partial^2\Delta p}{\partial t^2} = \nabla^2\Delta p,} \tag{17.5}$$

where we, for convenience, have introduced the constant,

$$c_0 = \sqrt{\frac{K_0}{\rho_0}}. \tag{17.6}$$

It has the dimension of a velocity and represents, as we shall see below, the *speed of sound* of harmonic waves. For water with $K_0 \approx 2.3$ GPa and $\rho_0 \approx 10^3$ kg m^{-3} the sound speed comes to about $c_0 \approx 1500$ m s^{-1} ≈ 5500 km h^{-1}.

Fluid	T ° C	c_0 m s^{-1}
Glycerol	25	1920
Sea water	20	1521
Fresh water	20	1482
Lube Oil	25	1461
Mercury	25	1449
Ethanol	25	1145
Hydrogen	27	1310
Helium	0	973
Water vapor	100	478
Neon	30	461
Humid air	20	345
Dry air	20	343
Oxygen	30	332
Argon	0	308
Nitrogen	27	363

Empirical sound speeds in various liquids (above) and gases (below). The temperature of the measurement is also listed. Data from various sources.

Isentropic sound speed in an ideal gas

Sound vibrations are normally so rapid that temperature equilibrium is never established, allowing us to assume that the oscillations locally take place adiabatically, i.e. without heat exchange. The bulk modulus of an isentropic ideal gas, eq. (2.45) on page 35, is $K_0 = \gamma p_0$ where γ is the adiabatic index, and we obtain

$$\boxed{c_0 = \sqrt{\frac{\gamma p_0}{\rho_0}} = \sqrt{\gamma R T_0}.} \tag{17.7}$$

In the last step we have used the ideal gas law in the form $p_0 = R\rho_0 T_0$ where $R = R_{\text{mol}}/M_{\text{mol}}$ is the specific gas constant (see eq. (2.27) on page 30).

Example 17.1 [Sound speed in the atmosphere]: For dry air at 20 ° C with $\gamma = 7/5$ and $M_{\rm mol} = 29$ g mol^{-1}, the sound speed comes to $c_0 = 343$ m s^{-1} $= 1235$ km h^{-1}. Since the temperature of the homentropic atmosphere falls linearly with height according to eq. (2.49) on page 36, the speed of sound varies with height z above the ground as

$$c = c_0 \sqrt{1 - \frac{z}{h_2}}, \tag{17.8}$$

where c_0 is the sound speed at sea level and $h_2 \approx 31$ km is the homentropic scale height. At the flying altitude of modern jet aircraft, $z \approx 10$ km, the sound speed has dropped to $c \approx 280$ m s^{-1} $\approx$ 1000 km h^{-1}. At greater heights this expression begins to fail because the homentropic model of the atmosphere fails.

Plane wave solution

An elementary plane pressure wave moving along the x-axis with wavelength λ, period τ and amplitude $p_1 > 0$ is described by a pressure correction of the form,

$$\Delta p = p_1 \sin(kx - \omega t), \tag{17.9}$$

where $k = 2\pi/\lambda$ is the wavenumber and $\omega = 2\pi/\tau$ is the circular frequency. Inserting this expression into the wave equation (17.5) , we obtain $\omega^2 = c_0^2 k^2$ or $c_0 = \omega/k = \lambda/\tau$. The surfaces of constant pressure (isobars) are planes orthogonal to the direction of propagation, satisfying the condition $kx - \omega t =$ const. Differentiating this equation with respect to time, we see that the planes of constant pressure move with velocity $dx/dt = \omega/k = c_0$, also called the *phase velocity* of the wave. This shows that c_0 given by (17.6) is indeed the speed of sound in the material.

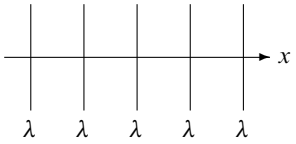

Plane pressure wave propagating along the x-axis with wavelength λ. There is constant pressure in all planes orthogonal to the direction of propagation.

From the x-component of the Euler equation (17.2) we obtain the only non-vanishing component of the velocity field

$$v_x = v_1 \sin(kx - \omega t), \qquad v_1 = \frac{p_1}{\rho_0 c_0} = \frac{p_1}{K_0} c_0. \tag{17.10}$$

Since $v_y = v_z = 0$, the velocity field of a sound wave in an isotropic fluid is always *longitudinal*, i.e. parallel to the direction of wave propagation. The corresponding spatial displacement field u_x, defined by $v_x = \partial u_x/\partial t$ becomes

$$u_x = a_1 \cos(kx - \omega t), \qquad a_1 = \frac{v_1}{\omega}, \tag{17.11}$$

where a_1 is the spatial displacement amplitude of the sound wave.

Validity of the approximation

It only remains to verify the approximation of dropping the advective acceleration. The actual ratio between the magnitudes of the advective and local accelerations is,

$$\frac{|(\boldsymbol{v} \cdot \boldsymbol{\nabla})\boldsymbol{v}|}{|\partial \boldsymbol{v}/\partial t|} \approx \frac{k v_1^2}{\omega v_1} = \frac{v_1}{c_0}. \tag{17.12}$$

The condition for the validity of the approximation is thus that *the amplitude of the velocity oscillations should be much smaller than the speed of sound*, $v_1 \ll c_0$. This is equivalent to $p_1 \ll K_0$, and to $ka_1 \ll 1$ or $a_1 \ll \lambda/2\pi$.

Example 17.2 [Loudspeaker]: A certain loudspeaker transmits sound to air at frequency $\omega/2\pi = 1000$ s^{-1} with diaphragm displacement amplitude of $a_1 = 1$ mm. The velocity amplitude becomes $v_1 = a_1\omega \approx 6$ m s^{-1}, and since $v_1/c_0 \approx 1/57$ the approximation of leaving out the advective acceleration is well justified.

17.2 Steady compressible flow

In steady compressible flow, the velocity, pressure and density are all independent of time, and the Euler equations take the simpler form,

$$\boxed{(\boldsymbol{v}\cdot\nabla)\,\boldsymbol{v} = \boldsymbol{g} - \frac{1}{\rho}\nabla p, \qquad \nabla\cdot(\rho\boldsymbol{v}) = 0.} \tag{17.13}$$

Here we shall, for simplicity, assume that the fluid obeys a barotropic equation of state, $p = p(\rho)$ or $\rho = \rho(p)$, leaving us with a closed set of five field equations for the five fields, v_x, v_y, v_z, ρ and p. In this section gravity will mostly be ignored.

Effective incompressibility

Ernst Mach (1838–1916). Austrian positivist philosopher and physicist. Made early advances in psycho-physics, the physics of sensations. His rejection of Newton's absolute space and time prepared the way for Einstein's theory of relativity. Proposed the principle that inertia results from the interaction between a body and all other matter in the universe.

First we shall demonstrate the claim made in the preceding section that *in steady flow a fluid is effectively incompressible when the flow speed is everywhere much smaller than the local speed of sound*. The ratio of the local flow speed $\boldsymbol{v}$ (relative to a static solid object or boundary wall) and the local sound speed c is called the (local) *Mach number*,

$$\boxed{\mathsf{Ma} = \frac{|\boldsymbol{v}|}{c}.} \tag{17.14}$$

In terms of the Mach number, the claim is that a steady flow is effectively incompressible when $\mathsf{Ma} \ll 1$ everywhere. Conversely, the flow is truly compressible if the local Mach number somewhere is comparable to unity or larger, $\mathsf{Ma} \gtrsim 1$.

The essential step in the proof is to relate the gradient of pressure to the gradient of density, $\nabla p = (dp/d\rho)\nabla\rho = c^2\nabla\rho$, where $c = \sqrt{dp/d\rho}$ is the local speed of sound. Writing the divergence condition in the form $\nabla\cdot(\rho\boldsymbol{v}) = \rho\nabla\cdot\boldsymbol{v} + (\boldsymbol{v}\cdot\nabla)\rho = 0$ and making use of the Euler equation without gravity, we find the exact result,

$$\nabla\cdot\boldsymbol{v} = -\frac{1}{\rho}(\boldsymbol{v}\cdot\nabla)\rho = -\frac{1}{\rho c^2}(\boldsymbol{v}\cdot\nabla)p = \frac{\boldsymbol{v}\cdot(\boldsymbol{v}\cdot\nabla)\boldsymbol{v}}{c^2}. \tag{17.15}$$

Applying the Schwarz inequality to the numerator (see problem 17.2) we get

$$\boxed{|\nabla\cdot\boldsymbol{v}| \le \frac{|\boldsymbol{v}|^2}{c^2}\,|\nabla\boldsymbol{v}| = \mathsf{Ma}^2\,|\nabla\boldsymbol{v}|\,,} \tag{17.16}$$

where $|\nabla\boldsymbol{v}| = \sqrt{\sum_{ij}(\nabla_i v_j)^2}$ is the norm of the velocity gradient matrix.

This relation clearly demonstrates that for $\mathsf{Ma}^2 \ll 1$ the divergence $\nabla\cdot\boldsymbol{v}$ is much smaller than the general size of the velocity gradients $\nabla\boldsymbol{v}$, making the incompressibility condition, $\nabla\cdot\boldsymbol{v} = 0$, a good approximation. Typically, a flow will be taken to be incompressible when $\mathsf{Ma} \lesssim 0.3$ everywhere, corresponding to $\mathsf{Ma}^2 \lesssim 0.1$.

Example 17.3 [Mach numbers]: Waving your hands in the air, you generate flow velocities at most of the order of meters per second, corresponding to $\mathsf{Ma} \approx 0.01$. Driving a car at 120 km h^{-1} $\approx$ 33 m s^{-1} corresponds to $\mathsf{Ma} \approx 0.12$. A passenger jet flying at a height of 10 km with velocity about 900 km h^{-1} $\approx$ 250 m s^{-1} has $\mathsf{Ma} \approx 0.9$ because the velocity of sound is only about 1000 km h^{-1} at this height (see example 17.1). Even if this speed is subsonic, considerable compression of the air must occur especially at the front of the wings and body of the aircraft. The Concorde and modern fighter aircraft operate at supersonic speeds at Mach 2–3, and the Space Shuttle enters the atmosphere at the hypersonic speed of Mach 25. The strong compression of the air at the frontal parts of such aircraft creates shock waves that appear to us as sonic booms.

Bernoulli's theorem for barotropic fluids

For compressible fluids, Bernoulli's theorem is still valid in a slightly modified form. If the fluid is in a barotropic state with $\rho = \rho(p)$, the Bernoulli field becomes,

$$H = \tfrac{1}{2}\boldsymbol{v}^2 + \Phi + w(p), \tag{17.17}$$

where

$$w(p) = \int \frac{dp}{\rho(p)} \tag{17.18}$$

is the *pressure potential*, previously defined in eq. (2.36) on page 32. The proof of the modified Bernoulli theorem is elementary and follows the same lines as before, using $Dw/Dt = (dw/dp)Dp/Dt = \rho^{-1}(\boldsymbol{v}\cdot\nabla)p$.

The most interesting barotropic fluid is an isentropic ideal gas with adiabatic index γ, for which it has been shown on page 36 that the pressure potential is linear in the temperature,

$$w = c_p\, T, \qquad\qquad c_p = \frac{\gamma}{\gamma-1}R, \tag{17.19}$$

where c_p is the specific heat of air and $R = R_{\text{mol}}/M_{\text{mol}}$ the specific gas constant. Thus, in the absence of gravity, a drop in velocity along a streamline in isentropic flow is accompanied by a rise in temperature (as well as a rise in both pressure and density).

Isentropic steady flow: There is a conceptual subtlety in understanding isentropic steady flow because of the unavoidable heat conduction that takes place in all real fluids. Since truly steady flow lasts "forever", one might think that there would be ample time for a local temperature change to spread throughout the fluid, regardless of how badly it conducts heat. But remember that steady flow is not static, and fresh fluid is incessantly being compressed or expanded adiabatically, accompanied by local heating and cooling. Provided the flow is sufficiently fast, heat conduction will have little effect. The physics of heat and flow will be discussed in chapter 22.

Stagnation temperature rise

An object moving through an ideal fluid has at least one stagnation point at the front where the fluid comes to rest relative to the object. There is also at least one stagnation point at the rear of a body, but vortex formation and turbulence will generally disturb the flow so much in this region that the streamlines get tangled and form unsteady whirls. This will often prevent us from using Bernoulli's theorem to relate velocity and pressure at the rear of the body.

At the forward stagnation point the gas is compressed and the temperature will always be higher than in the fluid at large (and similarly at the rear stagnation point if such exists). In the frame of reference where the object is at rest and the fluid asymptotically moves with constant speed and temperature, the flow is steady, and we find from the modified Bernoulli field (17.17) with pressure potential (17.19) in the absence of gravity,

$$\frac{1}{2}\boldsymbol{v}^2 + c_p T = c_p T_0, \tag{17.20}$$

where T_0 is the stagnation point temperature, and T is the temperature at a point of the streamline where the velocity is $\boldsymbol{v}$ (see the margin figure).

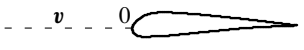

A static airfoil in an airstream coming in horizontally from the left. The pictured streamline (dashed) ends at the forward stagnation point.

The total temperature rise due to adiabatic compression thus becomes,

$$\boxed{\Delta T = T_0 - T = \frac{\boldsymbol{v}^2}{2c_p}.} \tag{17.21}$$

The stagnation temperature rise depends only on the velocity difference between the body and the fluid but not on the temperature, density or pressure of the gas. Note that a lower molar mass implies a higher specific heat and thus a smaller stagnation temperature rise.

Example 17.4: A car moving at 100 km h^{-1} has a stagnation temperature rise at the front of merely 0.4 K. For a passenger jet traveling at 900 km h^{-1} the stagnation temperature rise is a moderate 31 K, whereas a supersonic aircraft traveling at 2300 km h^{-1} suffers a stagnation point temperature rise of about 200 K. When a re-entry vehicle, such as the Space Shuttle, hits the dense atmosphere with a speed of 3 km s^{-1} the predicted stagnation point temperature rise would be 4500 K. At that temperature the air is dissociated and partly ionized, and becomes a glowing plasma with a much lower average molar mass (because of the larger number of low-mass particles in the plasma), and this lowers the stagnation temperature. The plasma also creates a hot shock front a small distance from the exposed surfaces which deflects most of the heat (see figure 26.7 on page 433). The surface temperatures do in fact not exceed 2500 K during reentry. Since such temperatures are nevertheless capable of melting and burning metals, it has been necessary to protect the exposed surfaces of the Space Shuttle with a special heat shield of ceramic tiles.

Stagnation and sonic properties

It is often convenient to express the ratio of the local temperature to the stagnation point temperature in terms of the local Mach number $\mathsf{Ma} = |\boldsymbol{v}|/c$ where $c = \sqrt{\gamma RT}$ is the local sound velocity. Setting $\boldsymbol{v}^2 = \mathsf{Ma}^2 c^2$ in eq. (17.20) we obtain

$$\boxed{\frac{T}{T_0} = \left(1 + \frac{1}{2}(\gamma - 1)\,\mathsf{Ma}^2\right)^{-1}.} \tag{17.22}$$

This relation is valid for any streamline because the stagnation temperature T_0 can be defined by means of eq. (17.20) , even if the streamline does not actually end in a stagnation point.

The corresponding pressure and density ratios are obtained from the isentropic relation, $T^\gamma p^{1-\gamma} = T_0^\gamma p_0^{1-\gamma}$, and the ideal gas law, $\rho = p/RT$,

$$\frac{p}{p_0} = \left(\frac{T}{T_0}\right)^{\gamma/(\gamma-1)}, \qquad \frac{\rho}{\rho_0} = \left(\frac{T}{T_0}\right)^{1/(\gamma-1)}. \tag{17.23}$$

In principle the stagnation values T_0, p_0, and ρ_0 can be different for different streamlines. But if for example an object moves through a homogeneous gas that is asymptotically at rest, all stagnation parameters will be true constants independent of the streamline. The flow is then said to be *homentropic*.

A point where the velocity of a steady flow equals the local velocity of sound, $v = c$, is analogously called a *sonic point*. The sonic temperature T_1, pressure p_1, and density ρ_1, are simply related to the stagnation values. Setting $\mathsf{Ma} = 1$ in the expressions above, we get

$$\frac{T_1}{T_0} = \frac{2}{\gamma + 1}, \qquad \frac{p_1}{p_0} = \left(\frac{T_1}{T_0}\right)^{\gamma/(\gamma-1)}, \qquad \frac{\rho_1}{\rho_0} = \left(\frac{T_1}{T_0}\right)^{1/(\gamma-1)} \tag{17.24}$$

For air with $\gamma = 7/5$ the right hand sides become $0.8333\ldots$, $0.5282\ldots$, and $0.6339\ldots$. The local to sonic temperature ratio may now be written

$$\frac{T}{T_1} = \left(1 + \frac{\gamma - 1}{\gamma + 1}\left(\mathsf{Ma}^2 - 1\right)\right)^{-1}, \tag{17.25}$$

from which the corresponding pressure and density ratios may be obtained using expressions analogous to (17.23) .

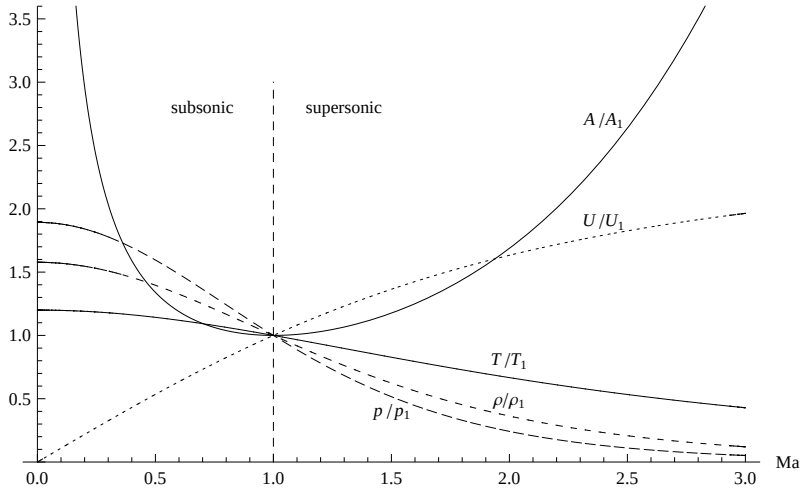

Figure 17.1. Plot of the ratio of local to sonic values as a function of the Mach number in a slowly varying duct for $\gamma = 7/5$. The ratio A/A_1 is a solid line, T/T_1 has large dashes, ρ/ρ_1 medium dashes, p/p_1 small dashes, and U/U_1 is dotted.

Duct with slowly varying cross section

Consider now an ideal gas flowing through a straight duct with a slowly varying cross section area $A = A(x)$ orthogonal to the x-axis (see the margin figure). The temperature T, density ρ, pressure p and normal velocity $U = v_x$ are assumed to be constant over any cross section, but like the area slowly varying with x. In this quasi-one-dimensional approximation we thus disregard the tiny flow components orthogonal to the x-axis. Since all streamlines have the same parameter values in any cross section, the flow is homentropic.

The constancy of the mass flow rate along the duct, $Q = \rho A U$, provides us with a useful relation between the duct area and the local Mach number. At the sonic point we have the same mass flow as everywhere else, so that $\rho A U = \rho_1 A_1 U_1$. Using $U/c = \mathsf{Ma}$ and $U_1/c_1 = 1$ where c and c_1 are the local and sonic sound velocities, we find

$$\frac{A}{A_1} = \frac{\rho_1 U_1}{\rho U} = \frac{1}{\mathsf{Ma}}\frac{c_1}{c}\frac{\rho_1}{\rho} = \frac{1}{\mathsf{Ma}}\left(\frac{T_1}{T}\right)^{1/2+1/(\gamma-1)},$$

where in the third step we used the ideal gas law. Finally, inserting (17.25) , we get,

$$\boxed{\frac{A}{A_1} = \frac{1}{\mathsf{Ma}}\left(1 + \frac{\gamma-1}{\gamma+1}\left(\mathsf{Ma}^2 - 1\right)\right)^{1/2+1/(\gamma-1)}}. \tag{17.26}$$

This function, which obviously has minimum $A = A_1$ at the sonic point $\mathsf{Ma} = 1$, is plotted as the solid curve in figure 17.1, together with the various flow parameters divided by their sonic values. Correspondingly, the current density of mass, $\rho U = Q/A$, can never become larger than the value it takes at the sonic point.

Figure 17.1 is central to the analysis of duct flow. Inspecting the curves we see that subsonic flow ($\mathsf{Ma} < 1$) follows the Venturi principle, such that a *decreasing* duct area implies *increasing* flow velocity and decreasing temperature, pressure and density (and conversely). But for supersonic flow ($\mathsf{Ma} > 1$) this behavior is reversed, such that an *increasing* duct area now leads to *increasing* velocity and decreasing temperature, pressure, and density (and conversely). This surprising behavior is the key to understanding how supersonic exhaust speeds are obtained in steam turbines, wind tunnels, supersonic aircraft and rocket engines.

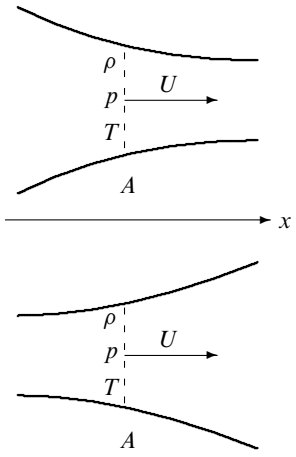

Top: Converging duct. For subsonic flow the velocity increases while the pressure decreases towards the right as in the Venturi effect. **Bottom:** Diverging duct. For supersonic flow the velocity increases while the pressure decreases towards the right.

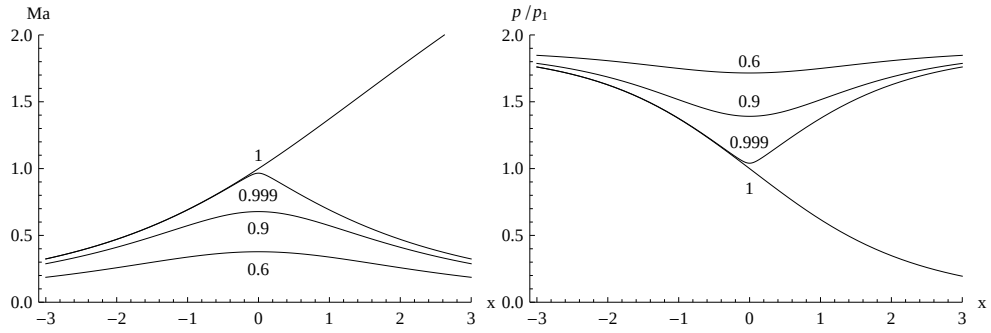

Figure 17.2. Simple symmetric model of a Laval nozzle, $A(x) = A_{\text{throat}} + kx^2$ for $-3 < x < 3$, with $A_{\text{throat}} = 1$ and $k = 0.1$ (and $\gamma = 7/5$). **Left:** Plot of the Mach number $\mathsf{Ma}(x)$ as a function of the duct coordinate x. The different curves are labeled with the ratio A_1/A_{throat}. **Right:** The pressure ratio $p(x)/p_1$ under the same conditions. For $A_1 < A_{\text{throat}}$, the pressure is lowest in the throat (the Venturi effect) but drops to much lower values for $A_1 = A_{\text{throat}}$ when the flow in the diverging part becomes supersonic. In this model the entry and exit Mach numbers are 0.32 and 2.14. The entry pressure is 9.0 times larger than the exit pressure.

Carl Gustav Patrik de Laval (1845–1913). Swedish engineer. Worked on steam turbines and dairy machinery, such as milk-cream separators and milking machines. In 1883 he founded a company which is now called Alfa Laval which still exists and is a world leader in heat transfer, separation and fluid handling. Discovered in 1888 that a converging-diverging nozzle generates much higher steam speed and thereby higher steam turbine rotation speed.

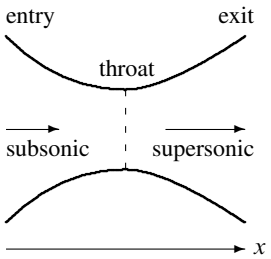

A subsonic flow may become supersonic in a duct with a constriction where the duct changes from converging to diverging. The transition must take place at the narrowest point of the nozzle, called the throat.

17.3 Application: The Laval nozzle

In 1888 the Swedish engineer *de Laval* discovered that supersonic steam speeds could be reached in steam turbines by accelerating the steam through a nozzle that first converges and then diverges, like the one shown in the margin figure and modeled in figure 17.2. This unique design has since been used in all kinds of devices, for example jet and rocket engines, in which one wishes to maximize thrust by accelerating the combustion gases to as high exhaust speed as possible.

The curves plotted in figure 17.1 indicate that the flow velocity will increase smoothly all the way through a converging-diverging duct, provided it passes through sonic speed precisely at the narrowest point, also called the *throat*. For this to happen, flow conditions must be arranged such that the sonic area exactly equals the physical throat area, $A_1 = A_{\text{throat}}$ (how this is done will be discussed below). Then, as the gas streams through the converging part of the nozzle, the local area A travels down the left-hand, subsonic branch of the area curve while the flow speed U simultaneously increases. Passing the throat at sonic speed, the gas streams through the diverging part while the local area travels up the right-hand supersonic branch and the speed continues to increase. Without the diverging part of the nozzle, the flow could at most reach sonic speed at the exit, but not go beyond. The expansion of the gas in the divergent part is thus essential for obtaining supersonic flow. In fact, the ratio of the nozzle's exit to throat area directly determines the Mach number of the exhaust.

Sonic speed is not always reached. Flutes and other musical instruments, including the human vocal tract, have constrictions in the airflow that do not give rise to supersonic flow (which would surely destroy the music). In this case the flow conditions must be such that the sonic area is strictly smaller than the physical throat area, $A_1 < A_{\text{throat}}$. As the gas streams through the converging part of the nozzle, its area travels as before down the left-hand branch of the area curve in figure 17.1 until it reaches the physical throat area where it turns around and backtracks up along the left-hand branch of the area curve while proceeding through the diverging part of the nozzle. The Mach number never reaches unity and the pressure rises until it passes the throat after which it falls back again in the exit region.

In fig. 17.2, a model of a Laval nozzle is solved for a few values of A_1/A_{throat}, including the unique *critical* solution, $A_1 = A_{\text{throat}}$, where the flow does become sonic right at the throat, and continues as supersonic afterwards. In this case the pressure continues to fall through the exit region.

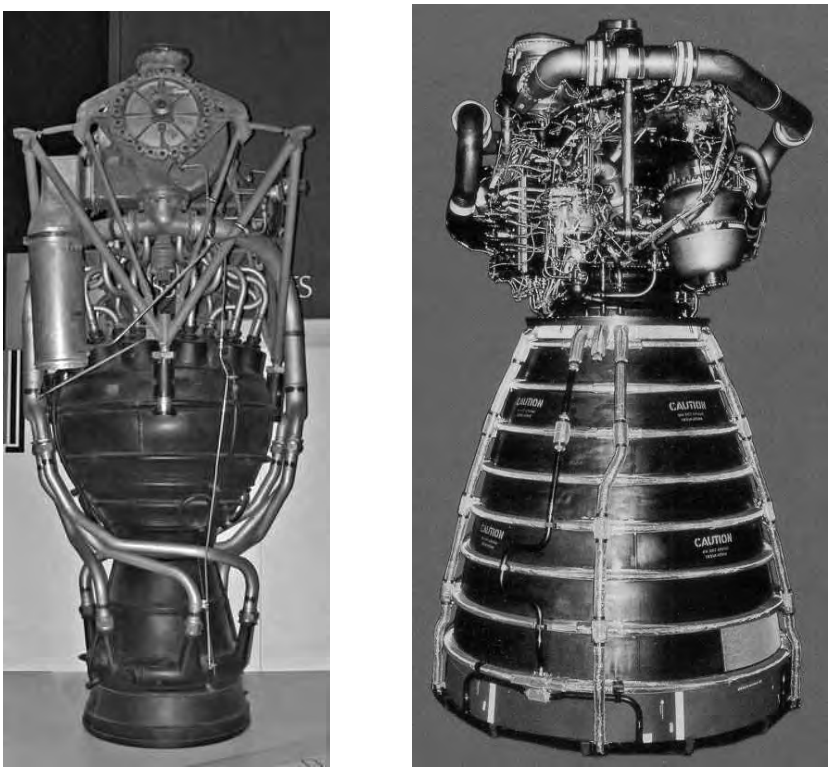

Figure 17.3. Left: A4/V2 rocket engine (cirka 1943). Developed and used by Germany during the Second World War. After the war it was used to "ignite" the American rocket program. Engine height: 1.7 meter. Propellant: 75% ethanol and liquid oxygen. The V2 rocket was powered by one such engine. Image courtesy Wikimedia Commons. **Right:** Space Shuttle Main Engine (SSME); developed in USA (cirka 1980). Engine height 4.3 meter. Propellant: liquid hydrogen and oxygen. The Space Shuttle was powered by three such engines, aided by two solid fuel boosters during lift-off. Image courtesy RocketDyne Archives (permission to be obtained).

Two rocket engines

Rocket engines, such as those in fig. 17.3, are controlled by the mass flow rate, Q, of propellant that enters the combustion chamber. The propellant is ignited and the resulting combustion gas streams at high temperature T_{entry} into a carefully shaped Laval nozzle, in which the speed becomes supersonic. We shall not discuss the complex transition from subsonic to supersonic flow during startup, but just assume that the engine is now running steadily with the sonic area equal to the throat area, $A_1 = A_{\text{throat}}$. Besides the nozzle geometry, $A = A(x)$, the mass flow rate Q, the entry temperature T_{entry}, we only need to know the average molar mass M_{mol} of the combustion gas and its adiabatic index γ. From these input values, the physical conditions may be calculated everywhere in the engine using the formalism established in the preceding subsection. The main results are shown in table 17.1 for the case of the two important engines pictured in fig. 17.3. We shall now outline the procedure.

The Mach number distribution, $\mathsf{Ma}(x)$, is calculated by solving eq. (17.26) numerically using the known area ratio $A(x)/A_{\text{throat}}$. In particular, the entry Mach number, $\mathsf{Ma}_{\text{entry}} < 1$, may be calculated from the entry-to-throat ratio, $A_{\text{entry}}/A_{\text{throat}}$, and the exit Mach number $\mathsf{Ma}_{\text{exit}} > 1$ from the exit-to-throat ratio, $A_{\text{exit}}/A_{\text{throat}}$. Since the Mach number only depends on the area ratio, engines with congruent geometry perform identically. Scaling up a rocket engine from model to full size is easy—at least in this respect.

Input values		
	A4/V2	SSME
A_{entry}	0.69 m^2	0.21 m^2
A_{throat}	0.13 m^2	0.054 m^2
A_{exit}	0.42 m^2	4.17 m^2
γ	1.2	1.2
M_{mol}	26.9 g/mol	14.1 g/mol
T_{entry}	3000 K	3600 K
Q	125 kg/s	494 kg/s

Output values		
	A4/V2	SSME
$\mathsf{Ma}_{\text{entry}}$	0.11	0.15
$\mathsf{Ma}_{\text{exit}}$	2.47	4.71
ρ_{entry}	1.54 kg/m^3	9.60 kg/m^3
p_{entry}	14.3 bar	204 bar
U_{entry}	117 m/s	239 m/s
T_{exit}	1865 K	1122 K
p_{exit}	0.83 Bar	0.19 bar
ρ_{exit}	0.14 kg/m^3	0.028 kg/m^3
U_{exit}	2055 m/s	4200 m/s
$\mathcal{R}$(1 bar)	250 kN	1737 kN
$\mathcal{R}$(0 bar)	292 kN	2154 kN

Table 17.1. Comparison of A4/V2 and SSME rocket engines. The average molar mass M_{mol} is calculated from the combustion chemistry. For the A4/V2 the fuel is a mixture of 75% ethanol and 25% water whereas for the SSME it is pure liquid hydrogen. In both engines the oxidizer is liquid oxygen. The engines run "fuel rich" which means that there is fuel left over in the combustion gas after all the oxygen has reacted. For the A4/V2 the exhaust gas becomes a mixture (by mass) of 56% carbon dioxide and 44% water (see problem 17.4), whereas for the SSME the mixture is 96.5% water and 3.5% hydrogen (see problem 17.5). The adiabatic index γ which by the usual rules should be about 4/3 (see appendix E) is actually more like 1.2 at these high temperatures.

Having determined the Mach number, $\mathsf{Ma}(x)$, the temperature $T(x)$ may now be calculated from eq. (17.24) with $T_1 = T_{\text{throat}}$. The unknown throat temperature T_{throat} is obtained from T_{entry} by setting $\mathsf{Ma} = \mathsf{Ma}_{\text{entry}}$ in this equation. From the temperature we obtain the local sound velocity, $c(x) = \sqrt{\gamma RT(x)/M_{\text{mol}}}$, and the flow speed, $U(x) = \mathsf{Ma}(x)\,c(x)$. The gas density $\rho(x) = Q/U(x)A(x)$ can now be calculated everywhere in the nozzle from the known mass flow. Finally, the pressure in the nozzle is determined by the ideal gas law, $p(x) = \rho(x)RT(x)/M_{\text{mol}}$. In table 17.1 the input and output values are shown for the two engines pictured in fig. 17.3.

The total reaction force from the exhaust gas (which is the force that accelerates the rocket) is called the *thrust*. In chapter 21 we shall systematically investigate reaction forces, but here it is fairly simple to write it down (see page 345),

$$\mathcal{R} = QU_{\text{exit}} + (p_{\text{exit}} - p_{\text{atm}})A_{\text{exit}}. \tag{17.27}$$

The first term is the rate at which momentum is carried away by the exhaust gases and thereby adding momentum to the rocket itself at the same rate. The second is the force due to the pressure difference between the exhaust gas and the ambient atmosphere. If the design goal is to obtain a particular thrust, this equation can instead be used to determine one other parameter, for example the mass flow rate. The predicted thrust for each of the two rocket engines is also shown in table 17.1 (for atmospheric pressure and for vacuum). Although the results are estimates, the calculated thrust agrees quite well with the quoted values.

Acceleration at lift-off: The initial mass of the V2 rocket was 12500 kilogram, and with a thrust of 250 kilonewton which equals twice the initial weight of the rocket, the lift-off acceleration became nearly equal to the acceleration due to gravity. The space shuttle is equipped with three main engines and two solid rocket boosters, each delivering 12.5 meganewton. With an initial mass of 2 million kilogram, the total thrust is 1.5 times the initial weight so that the Space Shuttle initially accelerates upwards with about half the acceleration due to gravity. During ascent the acceleration grows to several times gravity, partly because fuel is being spent and partly because the atmosphere becomes thinner which increases the thrust according to eq. (17.27) .

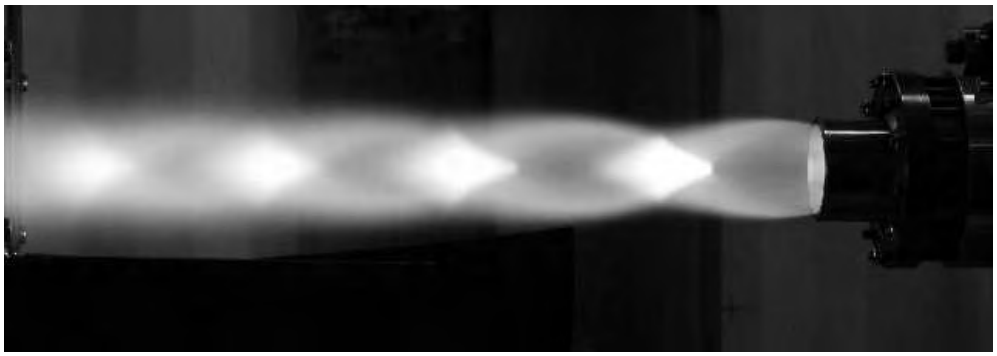

Figure 17.4. Beautiful shock diamonds formed in the exhaust from a small rocket engine with 2.5 kilonewtons thrust. Picture courtesy Swiss Propulsion Laboratory (permission to be obtained).

Why the pressure difference?

One may wonder why we allow for a difference between the exit pressure and the ambient pressure in eq. (17.27) . In the analysis of incompressible flow, for example Torricelli's law on page 212, we always assumed that the exit pressure was equal to the ambient. The reason is that in incompressible flow, any mismatch between exit and ambient pressure is instantly communicated to all of the fluid, as discussed in the comment on the non-locality of pressure on page 208.

In subsonic flow upstream communication is still possible, because the local speed of sound is larger than the local speed of the flow. But in the diverging part of a supersonic nozzle there is no way to communicate anything upstream by means of sound waves because the flow speed is everywhere larger than the local speed of sound. The nozzle entry is—so to speak—completely out of touch with what goes on at the exit. As a consequence, a nozzle running supersonic is said to be *choked* because it is not possible to increase the mass flow by lowering the ambient pressure or even applying active suction at the exit. There is, however, no injunction against increasing the mass flow simply by increasing the propellant pumping rate. Since $Q = \rho_{\text{entry}} U_{\text{entry}} A_{\text{entry}}$, this will for fixed entry temperature lead to an increase in the entry gas density, the entry pressure and thus in the exit pressure.

Shocks and diamonds

What actually happens at the exit because of the pressure difference is quite complicated (see for example [Anderson 2004, White 1999, Faber 1995]). If the exit pressure is higher than the ambient pressure, $p_{\text{exit}} > p_{\text{atm}}$, the gas is said to be *underexpanded*. A pattern of standing shock waves, called *shock diamonds* or *Mach diamonds*, will form in the exhaust plume after the nozzle exit. A spectacular case is shown in fig. 17.4 which clearly justifies the name. If, on the other hand, the exit pressure is lower than the ambient pressure, $p_{\text{exit}} < p_{\text{atm}}$, the exhaust gas is said to be *overexpanded*. A static shock front will then form inside the diverging part of the nozzle at a certain distance from the exit (see the margin figure). At the downstream side of the shock front the supersonic nozzle flow drops abruptly to subsonic speed and the pressure, density, and temperature all jump to higher values. As the now subsonic gas proceeds through the remainder of the diverging channel, the velocity will further decrease while the thermodynamic parameters increase in accordance with the subsonic branch of figure 17.1, until ideally the exit pressure matches the ambient pressure. A shock diamond will also form in the overexpanded case, if the exit pressure following the internal standing shock exceeds the ambient pressure. Shocks will be discussed in some detail in chapter 26.

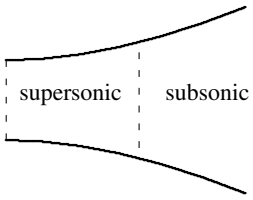

Static shock front in the diverging part of a Laval nozzle when the ambient pressure is higher than the exit pressure, such that the gas is overexpanded.

17.4 Dynamics of compressible Newtonian fluids

In deriving the Navier-Stokes equations for incompressible Newtonian fluids (14.20) on page 235, we explicitly used the vanishing of the velocity divergence, $\boldsymbol{\nabla} \cdot \boldsymbol{v} = 0$, to obtain the most general form (14.19) of a symmetric stress tensor that is linear in the velocity gradients. But when flow velocities become a finite fraction of the velocity of sound, it is—as discussed before—no longer possible to maintain the simplifying assumption of even effective incompressibility. For truly compressible fluids the divergence is non-vanishing, and we have to give up the simple divergence condition and replace it by the continuity equation (12.18) . In the same time it also opens the possibility for a slightly more general stress tensor.

Shear and bulk viscosity

The velocity divergence, $\boldsymbol{\nabla} \cdot \boldsymbol{v}$, is the only scalar field that can be constructed by linear combination of the velocity gradients, implying that the only term we can add to the stress tensor (14.19) must be proportional to $\delta_{ij} \boldsymbol{\nabla} \cdot \boldsymbol{v}$. Conventionally the proportionality constant is written $\zeta - \frac{2}{3}\eta$, where η is the shear viscosity, and ζ is a new material parameter, called *bulk viscosity* or the *expansion viscosity*. The complete stress tensor for a compressible isotropic Newtonian fluid in motion thus takes the form (Stokes, 1845),

$$\boxed{\sigma_{ij} = -p\,\delta_{ij} + \eta\left(\nabla_i v_j + \nabla_j v_i - \frac{2}{3}\,\boldsymbol{\nabla}\cdot\boldsymbol{v}\,\delta_{ij}\right) + \zeta \boldsymbol{\nabla}\cdot\boldsymbol{v}\,\delta_{ij}.} \tag{17.28}$$

Viewing this tensor as a first order expansion in the velocity field, it follows that p must be identified with the thermodynamic pressure, $p = p(\rho, T)$, of the fluid at rest.

Notice that the choice of proportionality constant makes the middle term traceless, so that the the mechanical pressure becomes $p_{\text{mech}} \equiv -\frac{1}{3}\sum_i \sigma_{ii} = p - \zeta\,\boldsymbol{\nabla}\cdot\boldsymbol{v}$. A viscous fluid in motion thus creates an extra *dynamic pressure*, $-\zeta \boldsymbol{\nabla}\cdot\boldsymbol{v}$, which is negative in regions where the fluid expands ($\boldsymbol{\nabla}\cdot\boldsymbol{v} > 0$) and positive where it contracts ($\boldsymbol{\nabla}\cdot\boldsymbol{v} < 0$). Bulk viscosity is hard to measure, because one must set up physical conditions such that expansion and contraction become important, for example by means of high frequency sound waves. In the following section we shall analyze viscous attenuation of sound in fluids, and see that it depends on both the shear and the bulk modulus. The measurement of attenuation of sound is quite complicated and yields a rather frequency-dependent bulk viscosity, although it may generally be assumed to be of the same overall magnitude as the coefficient of shear viscosity (see [DG09]).

The Navier–Stokes equations

Inserting the modified stress tensor (17.28) into Cauchy's equation of motion (12.33) on page 199, we obtain the field equation,

$$\boxed{\rho\left(\frac{\partial \boldsymbol{v}}{\partial t} + (\boldsymbol{v}\cdot\boldsymbol{\nabla})\boldsymbol{v}\right) = \boldsymbol{f} - \boldsymbol{\nabla} p + \eta\boldsymbol{\nabla}^2\boldsymbol{v} + \left(\zeta + \tfrac{1}{3}\eta\right)\boldsymbol{\nabla}(\boldsymbol{\nabla}\cdot\boldsymbol{v}).} \tag{17.29}$$

This is the most general form of the *Navier–Stokes equation*. Together with the equation of continuity (12.18) , which we repeat here for convenience,

$$\boxed{\frac{\partial \rho}{\partial t} + \boldsymbol{\nabla}\cdot(\rho\boldsymbol{v}) = 0,} \tag{17.30}$$

we have obtained four dynamic equations for the four fields v_x, v_y, v_z and ρ, while the pressure is determined by the thermodynamic equation of state, $p = p(\rho, T)$. For isothermal or isentropic flow the temperature is given algebraically, whereas in the general case we also need a differential *heat equation* to specify the dynamics of the temperature field (chapter 22).

Boundary conditions

The principal results of the discussion of boundary conditions for incompressible fluids on page 235 remain valid for compressible fluids, namely the continuity of the velocity field and the stress vector across an interface,

$$\Delta \boldsymbol{v} = \mathbf{0}, \qquad \Delta \boldsymbol{\sigma} \cdot \hat{\boldsymbol{n}} = \mathbf{0}. \tag{17.31}$$

The discussion of the continuity of pressure at a solid wall can, however, not be carried through to this case.

Shocks: In compressible inviscid fluids shock fronts may arise in which the flow parameters change abruptly (as mentioned in the preceding section and analyzed in detail in section 26.2). In such a shock the material is the same on both sides of the front, where low-density high-speed fluid on one side is converted to high-density low-speed fluid on the other. Viscosity does soften the discontinuity and replaces it by a very steep transition over a finite distance, but for high Reynolds number the thickness of the front is in fact so tiny that it approaches the smallest scale for the validity of the continuum approximation.

∗ Viscous dissipation

The rate of work against internal stresses is slightly more complicated in compressible fluids. Defining the shear strain rate,

$$v_{ij} = \frac{1}{2}\left(\nabla_i v_j + \nabla_j v_i - \frac{2}{3}\,\boldsymbol{\nabla}\cdot\boldsymbol{v}\,\delta_{ij}\right), \tag{17.32}$$

we obtain from eq. (7.38) on page 120 with $\delta\boldsymbol{u} = \boldsymbol{v}\,\delta t$ the following total rate of work against internal stresses,

$$\boxed{\dot{W}_{\text{int}} = \int_V \sum_{ij} \sigma_{ij}\nabla_j v_i \, dV = \int_V \left(-p\boldsymbol{\nabla}\cdot\boldsymbol{v} + 2\eta\sum_{ij} v_{ij}^2 + \zeta(\boldsymbol{\nabla}\cdot\boldsymbol{v})^2\right) dV.} \tag{17.33}$$

This expression reduces of course to the incompressible expression (14.23) on page 236 for $\boldsymbol{\nabla}\cdot\boldsymbol{v} = 0$. The first term in the integrand represents the familiar thermodynamic rate of work on the fluid because $\delta(dV) = \boldsymbol{\nabla}\cdot\boldsymbol{v}\,dV$ according to eq. (12.7) on page 193. As expected, it is positive during compression ($\boldsymbol{\nabla}\cdot\boldsymbol{v} < 0$) and negative during expansion, and may in principle be recovered completely under under quasistatic, adiabatic conditions. The last two terms are both positive and represent the work done against internal *viscous* stresses. They express the inevitable viscous dissipation of kinetic energy into heat.

∗ 17.5 Viscous attenuation of sound

It has previously (on page 232) been shown that free shear waves do not propagate through more than about one wavelength from their origin in any type of fluid. In nearly ideal fluids such as air and water, free pressure waves are capable of propagating over many wavelengths. Viscous dissipation (and many other effects) will nevertheless slowly sap their strength, and in the end all of the kinetic energy of the waves will be converted into heat.

In this section we shall calculate the rate of attenuation from damped small-amplitude solutions to the Navier–Stokes equations. The attenuation may equally well be calculated from the general expression for the dissipative work (17.33) ; see problem 17.8.

The wave equation

As in the discussion of unattenuated pressure waves in section 17.1 on page 281 we assume to begin with that a barotropic fluid is in hydrostatic equilibrium, $\boldsymbol{v} = \boldsymbol{0}$, without gravity, $\boldsymbol{g} = \boldsymbol{0}$, so that its density $\rho = \rho_0$ and pressure $p = p(\rho_0)$ are constant throughout space. Consider now a disturbance in the form of a small-amplitude motion of the fluid, described by a velocity field $\boldsymbol{v}$ which is so tiny that the nonlinear advective term $(\boldsymbol{v}\cdot\boldsymbol{\nabla})\boldsymbol{v}$ can be completely disregarded. This disturbance will be accompanied by tiny density corrections, $\Delta\rho = \rho - \rho_0$, and pressure corrections $\Delta p = p - p_0$, which we assume to be of first order in the velocity. Dropping all higher order terms, the linearized Navier–Stokes equations become,

$$\rho_0 \frac{\partial \boldsymbol{v}}{\partial t} = -\boldsymbol{\nabla}\Delta p + \eta\boldsymbol{\nabla}^2\boldsymbol{v} + \left(\zeta + \tfrac{1}{3}\eta\right)\boldsymbol{\nabla}(\boldsymbol{\nabla}\cdot\boldsymbol{v}), \tag{17.34a}$$

$$\frac{\partial \Delta\rho}{\partial t} = -\rho_0 \boldsymbol{\nabla}\cdot\boldsymbol{v}, \tag{17.34b}$$

$$\Delta p = c_0^2 \Delta\rho. \tag{17.34c}$$

where c_0 is the speed of sound (17.6) . Differentiating the last equation twice with respect to time and making use of the two first we obtain

$$\frac{1}{c_0^2}\frac{\partial^2 \Delta p}{\partial t^2} = \boldsymbol{\nabla}^2\Delta p + \frac{\zeta + \frac{4}{3}\eta}{\rho_0 c_0^2}\boldsymbol{\nabla}^2\frac{\partial \Delta p}{\partial t}. \tag{17.35}$$

If the last term on the right-hand side were absent, this would be a standard wave equation of the form (17.5) describing free pressure waves with phase velocity c_0. It is the last term which causes viscous attenuation, and its coefficient defines a characteristic viscous frequency,

$$\omega_0 = \frac{\rho_0 c_0^2}{\zeta + \frac{4}{3}\eta}. \tag{17.36}$$

The quantity $\zeta + \frac{4}{3}\eta$ is called the *longitudinal viscosity*.

Taking $\zeta \approx \eta$, the frequency scale becomes of the order of 3×10^9 s^{-1} in air at normal temperature and pressure, and about 10^{12} s^{-1} in water. In view of the huge values of the viscous frequency scale ω_0, the last term in eq. (17.35) will be small for frequencies that are much lower, $\omega \ll \omega_0$. Attenuation is, as we shall also see below, quite weak for normal sound, including ultrasound in the megahertz region.

Damped plane wave

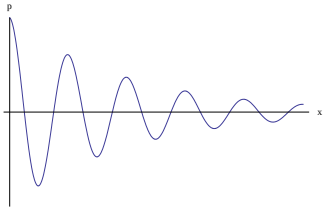

Damped pressure wave.

Let us assume that a wave is created by an infinitely extended plane, a "loudspeaker", situated at $x = 0$ and oscillating in the x-direction with a small amplitude at a definite circular frequency ω. The fluid near the plate has to follow the plate and will be alternately compressed and expanded, thereby generating a damped pressure wave of the form,

$$\Delta p = p_1 e^{-\kappa x}\sin(kx - \omega t), \tag{17.37}$$

where k is the wavenumber, and κ is the *viscous amplitude attenuation coefficient*, which determines the length scale for major attenuation. Inserting this wave into (17.35) , we get to first order in κ/k and ω/ω_0 the usual dispersion relation, $k = \omega/c_0$, and

$$\boxed{\kappa = \frac{\omega^2}{2\omega_0 c_0}}. \tag{17.38}$$

The viscous amplitude attenuation coefficient grows quadratically with the frequency, causing high frequency sound to be attenuated much more by viscosity than low frequency sound.

Example 17.5: In air at normal temperature and pressure, the viscous attenuation length $1/\kappa$ determined by this expression is huge, about 58 km, at a frequency of 1 kHz. At 10 kHz it is a hundred times shorter, about 580 m. Diagnostic imaging typically uses ultrasound between 1 and 15 MHz, but since living tissue is mostly water with higher density and sound velocity, the attenuation length is about 73 m at 10 MHz. At this frequency the calculated attenuation length in air is only 0.6 mm which is why the ultrasound emitter is pressed so very close to the skin (and the skin is lubricated with a watery gel).

The drastic reduction in attenuation length $1/\kappa$ with increased frequency is also what makes measurements of the attenuation coefficient much easier at high frequencies. From the viscous attenuation coefficient one may in principle extract the value of the bulk viscosity, but this is complicated by several other fundamental mechanisms that also attenuate sound, such as thermal conductivity, and excitation of molecular rotations and vibrations.

In the real atmosphere, many other effects contribute to the attenuation of sound. First, sound is mostly emitted from point sources rather than from infinitely extended vibrating planes, and that introduces a quadratic drop in amplitude with distance. Other factors like humidity, dust, impurities and turbulence also contribute, in fact much more than viscosity at the relatively low frequencies that human activities generate (see for example [Faber 1995, appendix] for a discussion of the basic physics of sound waves in real gases).

Problems

17.1 Show that for unsteady, compressible potential flow in a barotropic fluid with $\rho = \rho(p)$, the equations of motion may be chosen to be,

$$\frac{\partial \Psi}{\partial t} + \frac{1}{2}\boldsymbol{v}^2 + \Phi + w(p) = 0 \tag{17.39}$$

$$\frac{\partial \rho}{\partial t} + (\boldsymbol{v}\cdot\boldsymbol{\nabla})\rho = -\rho\boldsymbol{\nabla}^2\Psi \tag{17.40}$$

$$\tag{17.41}$$

where $\boldsymbol{v} = \boldsymbol{\nabla}\Psi$ and $w(p) = \int dp/\rho(p)$.

∗ **17.2** Use the Schwarz inequality

$$\left|\sum_n A_n B_n\right|^2 \le \sum_n A_n^2 \sum_m B_m^2 \tag{17.42}$$

to derive (17.16) .

∗ **17.3** Consider a non-viscous barotropic fluid in an external time-independent gravitational field $\boldsymbol{g}(\boldsymbol{x})$ with $\boldsymbol{\nabla}\cdot\boldsymbol{g} = 0$. Let $\rho_0(\boldsymbol{x})$ and $p_0(\boldsymbol{x})$ be density and pressure in hydrostatic equilibrium. **(a)** Show that the wave equation for small-amplitude pressure oscillations around hydrostatic equilibrium becomes,

$$\frac{\partial^2 \Delta p}{\partial t^2} = c_0^2\boldsymbol{\nabla}^2\Delta p - c_0^2(\boldsymbol{g}\cdot\boldsymbol{\nabla})\frac{\Delta p}{c_0^2}, \tag{17.43}$$

where c_0^2 is the local sound velocity in hydrostatic equilibrium. **(b)** Estimate under which conditions the extra term can be disregarded in standard gravity for an atmospheric wave of wavelength λ.

17.4 The A4V2 rocket engine propellant consists by mass of 43% ethanol (including 25% water) and 57% oxygen. The combustion reaction is $C_2H_5OH + 3O_2 \rightarrow 2CO_2 + 3H_2O$. Calculate the mixture of water and carbon dioxide in the exhaust gas and its molar mass. Estimate the power (rate of work) from the reaction enthalpy.

17.5 The SSME rocket engine propellant consists by mass of 14% hydrogen and 86% oxygen. The combustion reaction is $2H_2 + O_2 \rightarrow 2H_2O$. Calculate the mixture of water and hydrogen in the exhaust gas, and its molar mass. Estimate the power (rate of work) from the reaction enthalpy.

17.6 Calculate the isentropic pressure increase in a Pitot tube as a function of velocity.

17.7 Calculate the rate of dissipation per unit of volume of a planar wave using (17.33) .